Quantification of suction-driven flow of enhanced lateral drainage geotextiles

[1]Gino Sicha, M.S.,[2] Kangwei Chen, M.S.,[3] and Jorge Zornberg, P.h.D., P.E.[3]

[1]The University of Texas at Austin; e-mail: gino.sicha@utexas.edu
[2]Tongji University; e-mail: kwchen@tongji.edu.cn
[3]The University of Texas at Austin; e-mail: zornberg@mail.utexas.edu

ABSTRACT

Advances in geosynthetics have led to the development of geotextiles with enhanced drainage capabilities to allow suction-driven in-plane drainage of geotechnical and transportation systems. Specifically, fibers that incorporate grooves in their cross-section, referred to as "wicking fibers", have been developed to trigger enhanced drainage mechanisms. This paper presents the results of a theoretical and experimental evaluation of the in-plane flow of geotextiles with enhanced drainage capabilities conducted in isolation to assess the variables governing the flow magnitude. An analytical solution based on Lucas-Washburn's law was derived to predict flow in geotextile with enhanced drainage capabilities specimens. Additionally, horizontal drainage tests were conducted to assess the in-plane drainage behavior of geotextiles while avoiding moisture losses due to evaporation. These tests involved geotextiles positioned horizontally along a leveled surface, with one end of the geotextile submerged in a water reservoir and the other end allowed to drain freely. The flow rate was determined by measuring the wetted length over time. The flow model developed as part of this study was found to be useful for explaining and predicting the behavior of in-plane drainage of geotextiles with enhanced drainage capabilities under a high relative humidity.

INTRODUCTION

Geotextiles with enhanced drainage capabilities have been developed to facilitate drainage of soil layers that may be under unsaturated conditions and are placed in contact with the geotextile. While field and experimental evidence has been documented on the drainage capabilities of these new geosynthetic materials, quantification of the lateral drainage has been challenging as it depends on the laboratory conditions under which the geotextiles with enhanced drainage capabilities are tested. The present study focuses on the analytical prediction of spontaneous horizontal flow which consists of the generation of flow exerted only by the capillary force. External forces, such as pressure head, that could lead to a higher in plane-flow are not evaluated in this paper. The analytical prediction of spontaneous horizontal flow focuses particularly on geotextiles with enhanced drainage capabilities tested in isolation. Additionally, laboratory tests were performed to validate the analytical prediction of spontaneous horizontal flow.

THEORETICAL PREDICTION OF SPONTANEOUS HORIZONTAL FLOW

The geotextiles with enhanced drainage capabilities evaluated in this study are made of nylon wicking fibers in the cross-machine direction. A schematic of cross-section of a wicking fiber is shown in Figure1a. These nylon fibers are capable of transporting water through their grooves. The microscopic groves allow water along their entire length since they are not enclosed. Thus,

they can be characterized as open micro-channels. Figure 1b shows an electron microscope view of one nylon fiber. In the product considered in this investigation, each yarn involves approximately 150 fibers, creating a preferential path for water to flow. An electron microscope view of a yarn cross-section is shown in Figure 1c.

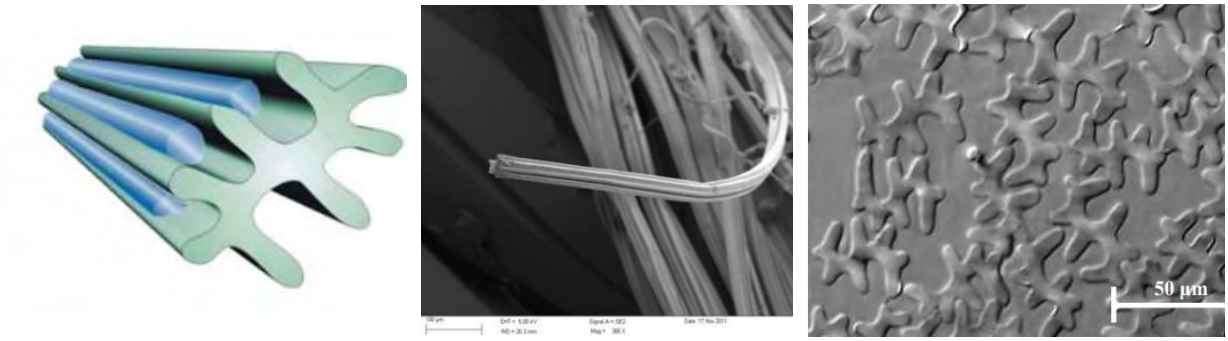

(a) (b) (c)

Figure 1. Wicking fibers in geotextiles with enhanced drainage capabilities used in this study: (a) schematic of grooved cross-section of a nylon fiber; (b) electron microscope view of in nylon fiber; (c) electron microscope view of cross-section of wicking yarns (Azevedo,2016).

To predict spontaneous horizontal capillary flow in geotextiles with enhanced drainage capabilities, the principle of flow in enclosed, cylindrical capillary tubes was studied based on a simplified model that follows Lucas-Washburn law (Berthier et al., 2019). Spontaneous capillary flow consists of the movement of a liquid in confined areas such as tubes with very small diameters. The liquid movement is triggered by the capillary force resulting from the intermolecular forces of the liquid and the liquid and the solid interaction. The intermolecular forces called “cohesive forces” are responsible for the bulk property of liquids and consists of the attractive forces between molecules of the same liquid. At the wetting front, the cohesive forces generate tension due to the liquid-air interaction which is called “surface tension” (De Gennes et al., 2002). On the other hand, the liquid-solid interactions identified in the technical literature as “adhesive forces” involve the attraction of the liquid to a solid (Berthier et al., 2019). At the wetting front, a concaved shape will be formed called “meniscus”. The concavity of the meniscus will depend on the relationship between cohesive and adhesive forces. The angle between the liquid and the solid at the meniscus is called contact angle (De Gennes et al., 2002). The principle of spontaneous horizontal capillary flow is presented in figure 2 showing the capillary forces generating water flow at the meniscus inclined by an angle theta which corresponds to the contact angle. For the theoretical analysis presented in this paper, the spontaneous horizontal flow of water was studied along a circular capillary tube made of nylon.

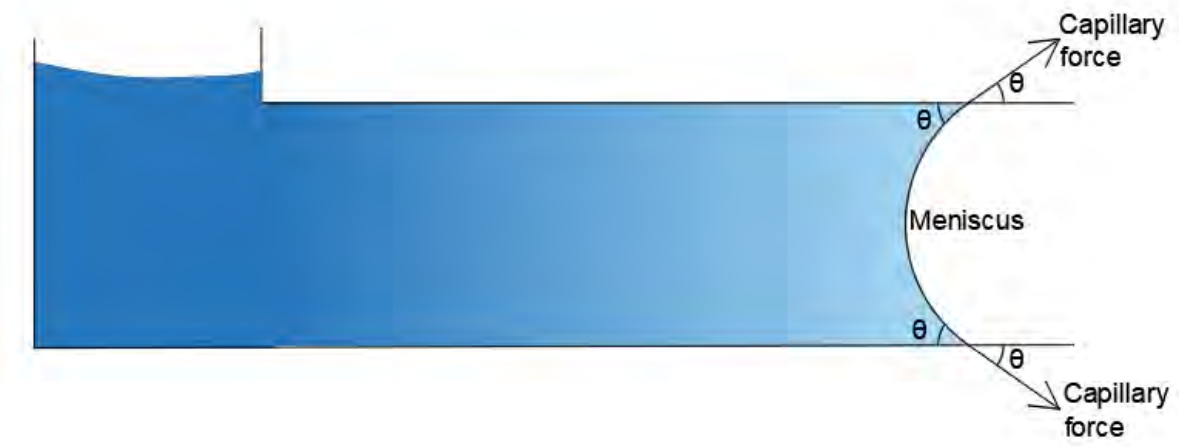

Figure 2. Principle of capillary pumping (based on Berthier and Brakke, 2012).

The flow from a water reservoir into an initially dry capillary tube placed horizontally involves two different regimes (Berthier et al, 2019). First, when water starts flowing through a dry capillary tube the inertial regime occurs. In this regime, an external force such as the capillary force is applied to the liquid forcing the liquid to flow though the capillary tube. The liquid will initially resist to a change in velocity or acceleration. The resistance to the movement of the matter, which is the liquid in this case, is called inertial force (Cohen and Whitman, 1999). After the wetting front has been initially mobilized, the friction between the liquid molecules and the inner walls of the capillary tube is called "viscous force" will increase and will start to prevail, while the inertial forces become negligible. This regime is called the viscous regime. Figure 3 presents a schematic of the location of the different regimes during spontaneous capillary flow. Lucas (1918) and Washburn (1921) derived an analytical prediction of horizontal flow in circular capillary tubes based on the assumption that the inertial forces are negligible focusing on the viscous regime. In this paper, the prediction of spontaneous horizontal flow is based on the Lucas-Washburn law (De Gennes et al., 2002). An additional force that is opposed to the movement is the air resistance, but it is typically neglected (Berthier et al, 2019).

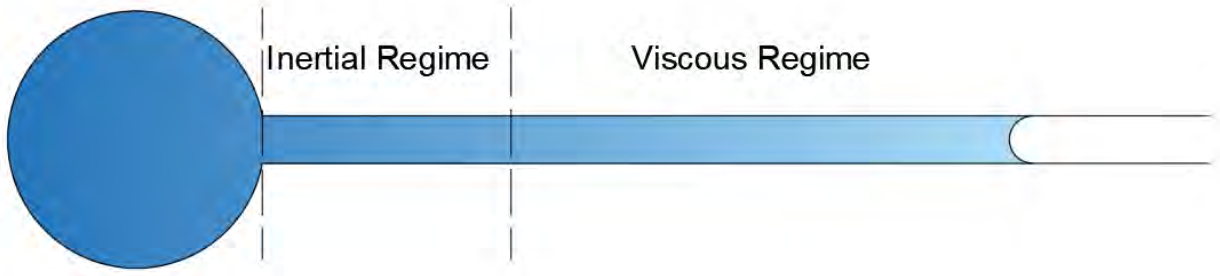

Figure 3. Inertial and viscous regime zones identified along a capillary tube during evolution of capillary flow (based on Berthier et al. 2019).

The driving force that causes the spontaneous driven flow in a capillary tube is called capillary force (F_c). It is related to the density of the liquid, contact angle, and radius of the tube. The driving force is defined in equation (1).

$$F_c = 2\pi R\gamma \cos\theta \ldots (1)$$

where:

R is the radius of the capillary tube;

θ is the contact angle; and

γ is the density of the fluid.

On the other hand, some forces resist the liquid movement. One such force, called inertial force, is negligible for this analysis, as previously stated, as the focus of this study is on the viscous regime zone of flow. Another such force, termed viscous force (F_v), is obtained from the Poiseuille profile for laminar flow in a cylindrical tube (Berthier et al, 2019). It is implicitly assumed that the flow travels following smooth paths in layers (laminar flow) and that the viscosity of the liquid does not depend on the shear stress (Newtonian liquid). Additionally, the velocity of the flow changes within the radius of the tube due to the friction with the tube, moving slower at the vicinity of the cylinder walls and achieving its maximum velocity at the center of the tube. The velocity gradient the liquid in the tube ($\frac{dv}{dr}$) and the resistance to movement between liquid layer paths called "dynamic or absolute viscosity" of the fluid (η) are used to determine the average wall friction per unit surface defined as $4\eta\frac{dv}{dr}$ (Berthier et al, 2019). This average wall friction per unit surface is defined along the total surface of the tube in contact with the liquid, which depends on the radius and wetted length of the tube ($2\pi Rz$). This means that as flow progresses, the viscous forces increase as well (De Gennes et. al., 2002). The viscous force is defined in equation (2).

$$F_v = (2\pi Rz)4\eta\frac{dv}{dr} \ldots (2)$$

The weight of the fluid (W) is also a resistant force, which means that it is opposed to the movement of the flow. Nevertheless, it only considered when the flow is vertical, but is neglected when flow is horizontal. The general flow equation, including the inertial force and weight, is:

$$\frac{d(MV)}{dt} = F_c - F_v - W \ldots (3)$$

As previously discussed, since the analysis focusses on the viscous regime, the inertial force of the fluid can be neglected in comparison to the viscous friction. Also, because the flow is horizontal, the weight of the fluid (gravity force) can be neglected. Thus, the flow equation can be simplified as follows:

$$F_c = F_v \ldots (4)$$

Replacing equations (1) and (2) in equation (4):

$$2\pi R\gamma \cos\theta = (2\pi Rz)4\eta \frac{dv}{dr} \ldots (5)$$

Thus:

$$\gamma \cos\theta \ dr = 4\eta z \ dv \ (6)$$

Since $dv = \frac{dz}{dt}$:

$$\frac{\gamma \cos\theta}{4\eta} dr = z \frac{dz}{dt} \ldots (7)$$

$$\int_0^t \int_0^R \frac{\gamma \cos\theta}{4\eta} drdt = \int_0^Z z \, dz \ldots (8)$$

Integrating:

$$\frac{\gamma R \cos\theta}{4\eta} t = \frac{z^2}{2} \ldots (9)$$

Rearranging the variables:

$$z^2 = \frac{\gamma R \cos\theta}{2\eta} t \ldots (10)$$

The following equation is known as Lucas-Washburn's law:

$$z = \sqrt{\frac{\gamma R \cos\theta}{2\eta}} \sqrt{t} \ldots (11)$$

The Lucas-Washburn's law establishes that the distance of the advancing liquid front is directly proportional to the square root of time. This means that the liquid progresses quickly at the beginning of the flow process, and it later slows down. Since the fibers in geotextiles with enhanced drainage capabilities are not actually straight, a tortuosity factor was included in the flow prediction to account for this characteristic (Azevedo, 2016). Tortuosity is inversely proportional to the movement of flow. Thus, equation (11) was modified to incorporate the tortuosity of the fibers as shown next:

$$z(t) = \sqrt{\frac{\gamma R \cos\theta}{2\eta\tau^2}} \sqrt{t} \ldots (12)$$

By getting the derivative of the previous equation, the velocity of the wetting front was determined as a function of time, as follows:

$$\frac{d\,z(t)}{dt} = v(t) = \sqrt{\frac{\gamma R\cos\theta}{4\eta\tau^2}}\frac{1}{\sqrt{t}} \ldots (13)$$

To predict flow along the wetting front, Darcy's law can be used as follows:

$$Q = v(t)A = \pi R^2\sqrt{\frac{\gamma R\cos\theta}{4\eta\tau^2}}\frac{1}{\sqrt{t}} \ldots (14)$$

The velocity of the advancing liquid, in terms of the distance of the wetting front (wetted length), can also be obtained as follows:

$$v(z) = \frac{\gamma}{\eta}\frac{R}{4\tau^2 z(t)}cos\theta \ldots (15)$$

The velocity versus distance equation demonstrates that the velocity of a liquid in a horizontal capillary tube is inversely proportional to the length of the tube, indicating that the flow will slow as the liquid advances.

Based on the equations (12), (13), (14) and (15), a theoretical prediction of spontaneous horizontal flow was made. The actual values of the different variables adopted in this study to predict the wetting front in the wicking fibers are those shown in Table 1. It should be noted that the wicking fibers do not have a cylindric transversal section, which is the assumed shape in the adopted theory. Nevertheless, this paper assumes that flow through the grooves in the wicking fibers can be represented by the water flows through a cylindrical tube of a given equivalent diameter. Consequently, the inner diameter of the equivalent cylindrical tube was back calculated based on the experimental data presented later in this paper. The objective of using the theoretical model was to establish a theoretical framework to establish the flow though geotextiles with enhanced drainage capabilities as well as the relevant variables that govern such flow.

Table 1. Variables used for theoretical prediction of horizontal flow.

Symbols	Variables	Value
θ	Contact angle	60°
d	Capillary tube diameter	$3.5\text{x}10^{-5}$ m
η	Fluid viscosity	$8.9\text{x}10^{-4}$ Pa.s
τ	Tortuosity	1.2
γ	Surface tension	0.045 N/m

Note: The contact angle, tortuosity and surface tension were extracted from Azevedo (2016).

The results obtained from the theoretical evaluation of spontaneous horizontal flow are presented in Figure 4. The distance advanced by the wetting front away from the water reservoir in relation to time (Lucas-Washburn law) was predicted using equation (12) and plotted in Figure 4a. The liquid was predicted to advance rapidly initially and then decrease its velocity. This reduction in velocity over time is due to the increase of the viscous force over the length of the capillary tube model. The reduction of velocity can be explained mathematically as well since the distance of the wetting front in equation (12) is proportional to the square root of time. Thus, the rate of the distance covered by the wetting front reduces gradually in time as shown in Figure 4a. Figure 4b shows how the time-dependent flow velocity decreases, which is particularly significant at the beginning. Equation (13) was used for the prediction of velocity over time. In Figure 4c, the velocity of the wetting front over the length of the geotextile is presented by using equation (14), indicating a considerable drop in velocity, as predicted. In Figure 4d, velocity was converted to flow using Darcy's law to quantify the number of liters being drained per day per feet by using equation (15).

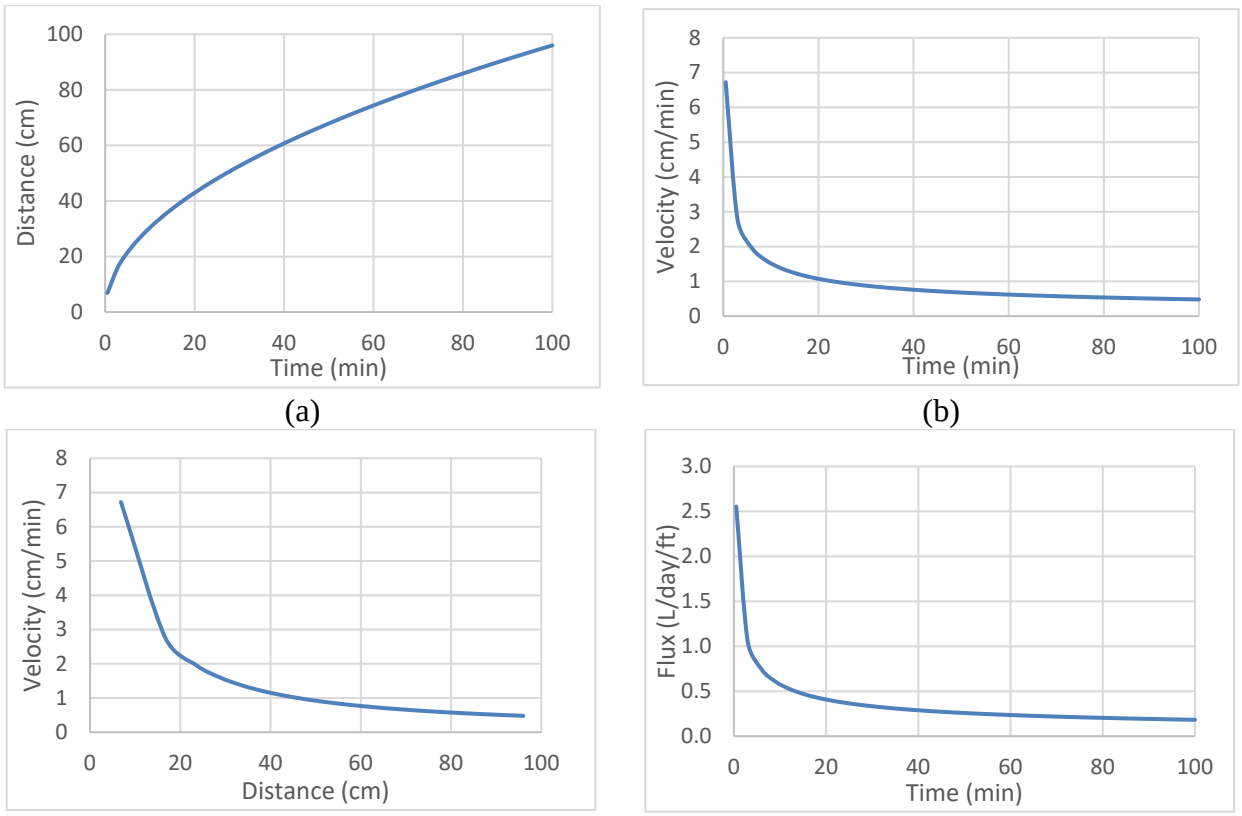

Figure 4. Prediction of spontaneous horizontal flow in geotextiles with enhanced drainage capabilities: (a) distance versus time; (b) velocity versus time; (c) velocity versus distance; and (d) flux versus time.

EXPERIMENTAL RESULTS OF SPONTANEOUS HORIZONTAL CAPILLARY FLOW

To validate the theoretical prediction of flow, a series of horizontal drainage tests were conducted to quantify the spontaneous horizontal flow of geotextiles with enhanced drainage capabilities at the wetting front. Other researchers, such as Azevedo (2016) and Guo (2017), have also reported results for similar tests.

The materials used for the horizontal drainage tests conducted in this study include: a water reservoir; 20-cm-wide by 1-m-long geotextile with enhanced drainage capabilities; ruler; hygrometer; humidifier; UV light; water dye; test box, also referred to as "environmental box;" and stopwatch.

Testing involved placing an end of the geotextile with enhanced drainage capabilities inside the water reservoir, while leaving the opposite end exposed to the atmosphere. The geotextile was positioned horizontally throughout testing, as displayed in Figure 5a. Tests were carried out in a sealed environmental box in which the temperature and relative humidity were controlled to prevent evaporation of water from the open micro-channels of the wicking fibers. A humidifier was placed inside the environmental box to maintain a relative humidity close to 100%. Keeping a high relative humidity is a crucial part of this testing setup since evaporation could reduce considerably the velocity of the wetting front. Thus, this test under lower relative humidity might not be in good agreement with the theoretical analysis presented previously due to the assumption considered for the derivation of the flow equations (12), (13), (14) and (15). Finally, a yellow dye was added to the water in the reservoir to facilitate easy identification of the wetting front using UV lights, as pictured in Figure 5b. Time and wetted length were recorded throughout testing.

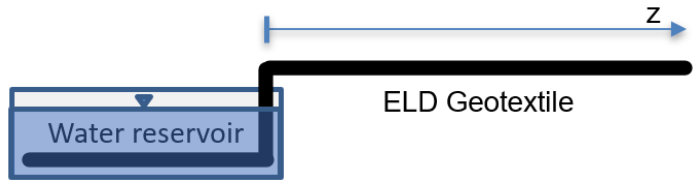

(a)

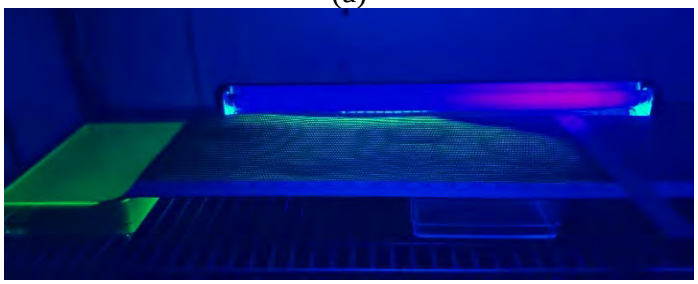

(b)

Figure 5. Horizontal drainage test setup: (a) layout of test setup; and (b) image of advancing wetting front during testing.

The results obtained from a series of five tests (repeats) performed under the same conditions are shown in Figure 6. Distance versus time is plotted in Figure 6a, showing the results of the 5 tests as well as the average values. It is revealed that the flow stopped after approximately 100 minutes. Figure 6b only shows the average data. It is observed a considerable decrease in velocity of the wetting front over time. Figure 6c presents the average velocity from the five tests performed in terms of wetted length. A significant decrease in velocity was observed along the initial 10 cm to 20 cm, beyond which the flow velocity continued decreasing, but at a much lower rate. In Figure 6d, the average velocity of the wetting front from the five tests was converted to water flow by estimating the cross-sectional area of the capillary tubes contained in the geotextile tested.

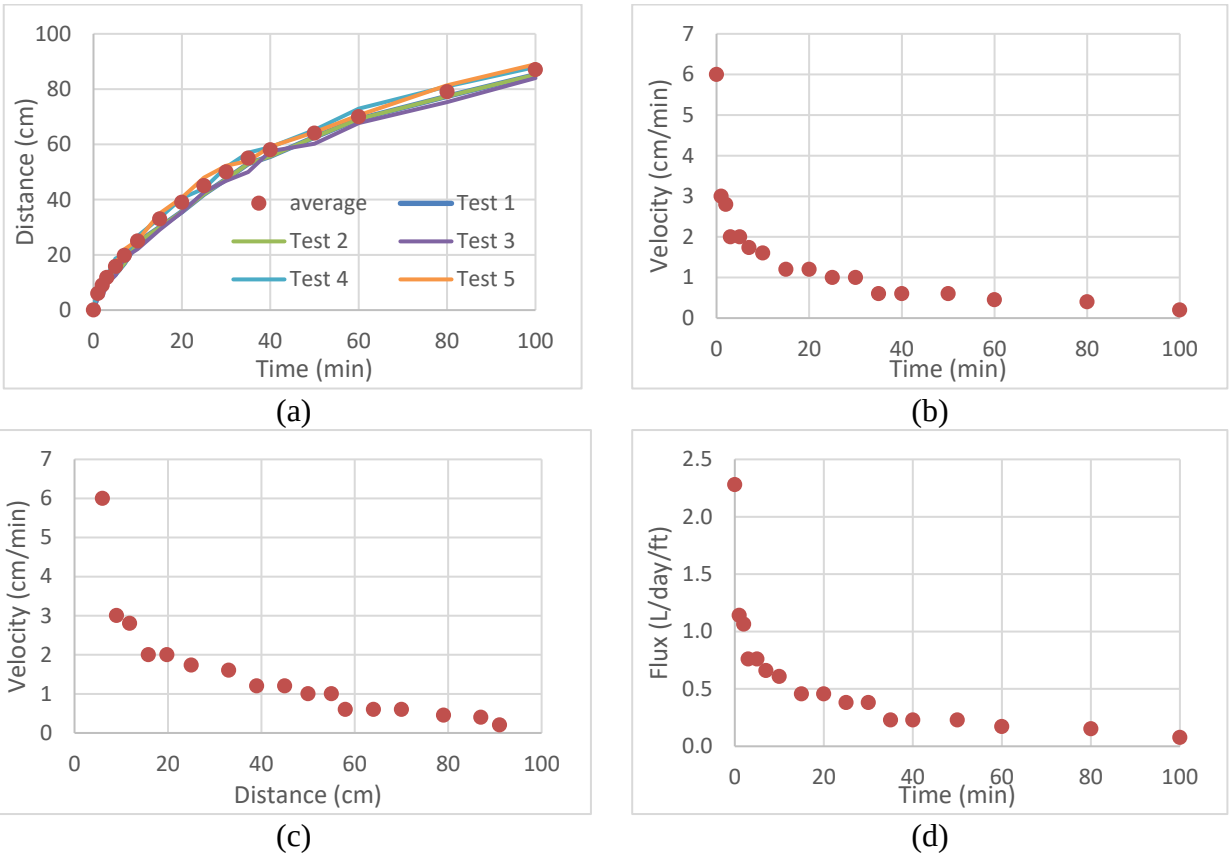

Figure 6. Experimental results from horizontal drainage tests: (a) distance versus time; (b) velocity versus time; (c) velocity versus distance; and (d) flux versus time.

COMPARISON BETWEEN EXPERIMENTAL AND PREDICTED RESULTS

A comparison was made between the analytical predictions and experimental results. Data from both analyses analytical and average values of the experimental results are plotted together in Figure 7. Figure 7.a shows the plot of the distance over time of both analyses. The prediction seems to slightly overpredict the flow particularly after 60 minutes. Figure 7.b plots the velocity against time. In this case both analyses seem to be overlapped. Figure 7.c plots the velocity again distance. In this case overlapping results of both analyses are observed as well. Lastly, Figure 7.d shows the flux over time, presenting matching results from both theoretical and analytic analyses. Thus, the

theoretical model and the laboratory tests seemed to be in agreement with each other. It should be noted that the equivalent diameter adopted in the prediction of flow through the wicking fibers was obtained through back calculation using data from figure 6. However, once such diameter was established, the trends of the different variables (distance, velocity, flux) was adequately predicted by the model. The results showed that the simplified theoretical model assuming enclosed capillary tubes with a circular cross-sectional area accurately predicted flow through more complex, open micro-channels, such as wicking fibers under high relative humidity (>95%). Nevertheless, tests conducted at a lower relative humidity might require other theoretical models that consider evaporation rate and/or open cross-sectional areas.

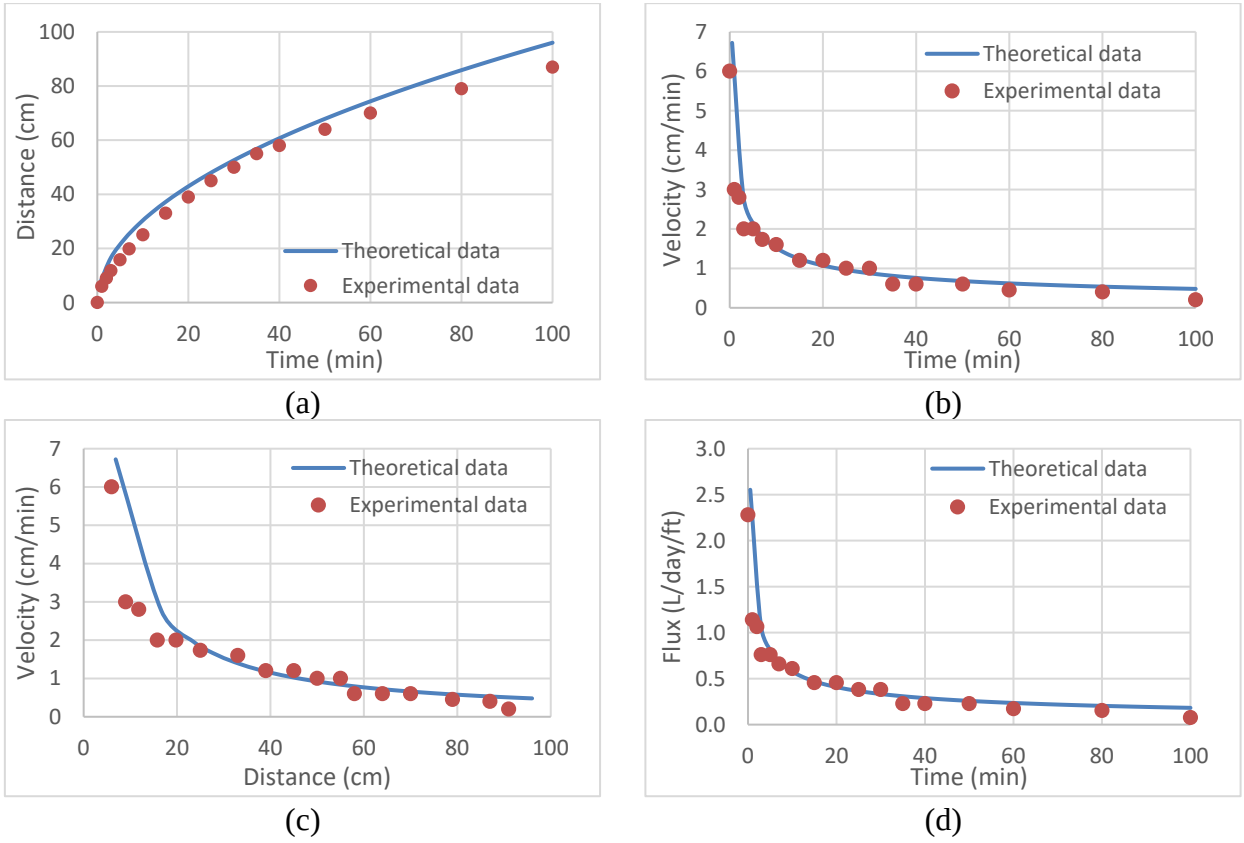

Figure 7. Comparison of theoretical and experimental results: (a) distance versus time; (b) velocity versus time; (c) velocity versus distance; and (d) flux versus time.

CONCLUSION

The quantification of the lateral drainage provided by geotextiles with enhanced drainage capabilities can be challenging because results may vary depending on the laboratory conditions under which geotextiles with enhanced drainage capabilities are tested. This paper focused on the prediction of the spontaneous horizontal flow rate of a geotextile enhanced drainage capabilities in isolation. A theoretical prediction was derived based on Lucas-Washburn law and a series of horizontal drainage tests were conducted to validate the flow prediction. Good agreement was observed between the theoretical prediction of flow and experimental data under a high relative

humidity (>95%). However, for cases in which evaporation is likely, more complex flow predictions that consider evaporation rate and/or open micro-channels models might be needed to accurately predict spontaneous horizontal flow in geotextiles enhanced drainage capabilities.

ACKNOWLEDGEMENTS
The authors gratefully acknowledged the financial support provided by TenCate Geosynthetics to this research.

REFERENCES

Azevedo, M. (2016), *Performance of Geotextiles with Enhanced Drainage.*, The University of Texas, Austin,Texas, USA.

Berthier, J., and Brakke, K. A. (2012), *The physics of microdroplets.*, Scrivener Publishing LLC, Hoboken, New Jersey, USA.

Berthier, J., Theberge, A. B., & Berthier, E. (2019), *Open-Channel Microfluidics Fundamentals and applications.*, Morgan and Claypool, Washington, Seattle, USA.

Cohen, B., & Whitman, A. (1999), *Isaac Newton The Principia Mathematical principles of natural philosophy.*, The Regents of the University of California, Oakland, California, USA.

De Gennes, P.-G., Brochard-Wyart, F., & Quere, D. (2002), *Capillarity and Wetting Phenomena: Drops, pearls, waves.*, Springer, Paris, Île-de-France, France.

Guo, J. (2017), *Evaluation and design of wicking Geotextiles for Pavement Applications.*, University of Kansas, Lawrence, Kansas, USA.

Lucas, R. (1918), Ueber das Zeitgesetz des Kapillaren Aufstiegs von Flussigkeiten., *Colloid and Polymer Science*, *23*,15-22.

Washburn, E. W. (1921), The Dynamics of Capillary Flow. *Physical Review*, *17*(3), 273-283.